AD-A119 094 ROYAL AIRCRAFT ESTABLISHMENT FARNBOROUGH (ENGLAND) F/G 20/4
CALCULATIONS OF ASYMMETRIC SEPARATED FLOW PAST CIRCULAR CONES A--ETC(U)
JUN 82 S P FIDDES, J H SMITH
UNCLASSIFIED RAE-TM-AERO-1949 DRIC-BR-84101 NL

END
DATE FILMED
10 82
DTIC

TECH. MEMO
AERO 1949

TECH. MEMO
AERO 1949

ROYAL AIRCRAFT ESTABLISHMENT

CALCULATIONS OF ASYMMETRIC SEPARATED FLOW PAST CIRCULAR CONES AT LARGE ANGLES OF INCIDENCE

by

S. P. Fiddes
J. H. B. Smith

June 1982

ROYAL AIRCRAFT ESTABLISHMENT

Technical Memorandum Aero 1949

Received for printing 25 June 1982

CALCULATIONS OF ASYMMETRIC SEPARATED FLOW PAST CIRCULAR CONES AT LARGE ANGLES OF INCIDENCE

by

S. P. Fiddes

J. H. B. Smith

Paper to be presented at the AGARD FDP Symposium on Missile Aerodynamics, Trondheim, Norway, 20-22 September 1982.

SUMMARY

The results of calculations of the flow over slender circular cones at large angles of incidence are presented. The vortices which form above the cone as a result of boundary-layer separation are represented by two inviscid models: as isolated line-vortices and as vortex sheets with line-vortex cores. For each model, an essentially new family of solutions is revealed, in which the flow remains asymmetric even when the separation lines are specified to lie symmetrically about the incidence plane. The side force which is predicted by this second family of solutions is very much larger than the side force which can be obtained by specifying asymmetric separation lines in the first family of solutions, and corresponds to the maximum side-force levels found experimentally. It is concluded that an essentially inviscid mechanism for the generation of side force at zero yaw has been discovered.

LIST OF SYMBOLS

C_p	pressure coefficient
C_Y	side-force coefficient
C_N	normal-force coefficient
i	$\sqrt{-1}$
r	radius
U	freestream speed
x,y,z	Cartesian body axis system (with perturbation velocities u, v, w)
Z	complex coordinate (= y + iz)
α	angle of incidence
Γ	circulation
δ	semi-apex angle of cone
θ	angular coordinate

subscripts

1,2	right hand, left hand
1,2,3,4,5	complex planes in transformation sequence
L,R	left, right (vortices)

1 INTRODUCTION

This paper is concerned with the out-of-plane force, or the side force at zero yaw, which arises on slender bodies at large angles of incidence. Space does not permit a detailed review of the phenomenon, but reference may be made to the recent account by Ericsson and Reding[1], and to the papers they cite. There is at present no general agreement about the mechanism responsible for the creation of out-of-plane forces, and, indeed, more than one mechanism may be involved in the whole range of body shapes, angles of incidence, Mach number and Reynolds number at which this phenomenon is observed. However, there is agreement that the phenomenon is associated with flow separation from these bodies, and that the detailed shape of the nose of the body has a strong influence. In general terms, at a sufficiently large angle of incidence, the flow on the body surface diverges from an attachment line on the windward side and separates along two lines on the sides of the body. The shear layers which spring from the separation lines roll up into a pair of contra-rotating vortices which lie above the body.

We shall only concern ourselves with pointed bodies of revolution at angles of incidence for which the separation lines extend forward to the pointed nose. In these circumstances, the vortices form at the nose, and their initial development is the same as it would be on a circular cone. For a certain range of incidence, the flow is always found to be symmetric, but at larger incidences, asymmetric flows are observed. In particular, the two separation lines on the surface are not symmetrically placed about the incidence plane and the two vortices also lie in asymmetric positions. The question arises whether it is the asymmetry in the separation line positions that causes the asymmetry in the vortices, or the asymmetry in the vortices that causes the asymmetry in the separation lines. There is, of course, a sense in which it is inappropriate to speak of cause and effect, but we believe the evidence presented here will show that there is an inherent asymmetry in the inviscid flow to which the viscous flow, and hence the separation positions, must adjust. In other words, the essential mechanism responsible for the out-of-plane forces is an inviscid one.

Evidence for this will be given in the form of results of calculations using two simple inviscid models of the flow past a circular cone at incidence, together with some recent measurements made at RAE by Mundell[2]. Since the theoretical models are inviscid, the positions of the separation lines are specified at the start of the calculation. In principle, the separation positions could also be predicted for laminar flows, using the method described in an earlier paper by Fiddes[3] for symmetric flows. However, we have exploited the freedom to specify the separation positions.

In the first place, we have started with a previously known solution for the symmetric flow past a circular cone, in which the separation position has been specified symmetrically. This solution has then been modified progressively by introducing a gradually increasing asymmetry in the separation lines. This gives rise to a moderate degree of asymmetry in the vortices, as regards their positions and circulations, and also produces a side force. However, even for a large asymmetry in the positions of the separation lines, the side force remains a small proportion of the normal force, whereas measured values of the side force are known to approach the magnitude of the normal force. This leads us to believe that the phenomenon is not being driven by a boundary layer mechanism, such as differential transition.

In the second place, we have specified symmetric separation line positions on the circular cone and found a family of solutions in which the vortices are asymmetric. Results have already been published[4] for the simpler of the two mathematical models considered in which the vortices are represented by line vortices joined to the separation lines by cuts (a model first used for the symmetrical flow past bodies by Bryson[5]). New results have been obtained for the more realistic model, described for symmetric flows by Fiddes[3], where the shear layers are represented by vortex sheets, which offer further evidence for this non-uniqueness of the inviscid flow. With these symmetric separation lines, substantial flow asymmetry is still possible and side forces similar in magnitude to the normal force are predicted. This means that there is an inviscid mechanism which is capable of producing the observed levels of side force with no appeal to viscous effects.

Of course, the real separation lines are not symmetrically placed, so the third step has been to take the observed separation positions from an experiment and supply them to the inviscid model in order to calculate the side force. As indicated above, if the solutions are of the first family, in which the solution reverts to its symmetrical form when the separation lines are symmetric, the side force calculated is small, much smaller than that observed in the experiment. On the other hand, if the solutions are taken from the second family, which remain asymmetric even with symmetric separation lines, the calculated side force agrees quite closely with the measured value.

2 MATHEMATICAL MODELS OF THE FLOW

The simpler of the models used is an extension of the line-vortex model of Bryson[5]. The more complex model is a development of the inviscid component of the method described in Ref 3. The more complex model used is described first, followed by the simplifications that reduce it to an extension of Bryson's model.

The free shear layers are represented by vortex sheets, with the inner turns of each vortex sheet replaced by an isolated line-vortex. The isolated line-vortex represents the core, and is joined to the free end of the vortex sheet by a cut as indicated for the starboard vortex in Fig 1. Boundary conditions are applied on the sheet, such that it is a stream-surface of the three-dimensional flow sustaining no pressure jump. The conditions applied to each line-vortex and cut are that the combination is force-free. A condition analogous to a Kutta condition is applied at the separation line. The vortex sheet model used is essentially that described by Smith[6], apart from differences in discretisation and details of the Kutta condition. As in Ref 3, the assumptions of slender-body theory and conical flow are still used, but the flow is, of course, no longer symmetrical. The slenderness assumption reduces the problem to the solution of the two-dimensional Laplace equation in each cross-flow plane, with appropriate boundary conditions on the vortex sheets and cone surface. The assumption that the flow is conical means that we need only find the solution in one cross-flow plane. Conformal transformation techniques are used to simplify the solution of the resulting boundary-value problem. The mappings used in Ref 3 relied on the lateral symmetry of the flow so this means that a different approach must be adopted for the construction of the complex potential describing the asymmetric flow in a cross-flow plane. A new transformation sequence results.

The velocity field is linear in its components. Fig 2 shows the decomposition of this field into the contributions arising from:

(a) the displacement effect of the growth of the cone cross-section along its length

(b) the angle of incidence (or incidence plus yaw) of the cone

(c) the isolated vortices representing the inner parts of the rolled up vortex sheet

(d) the outer part of the vortex sheets.

Since the cross-section of the cone is circular, the contributions of (a), (b) and (c) to the velocity field can be written down at once as:

$$v - iw = \frac{\delta U r}{z} - i\alpha U\left(1 + \frac{r^2}{z^2}\right) + \frac{\Gamma_L}{2\pi i}\left[\frac{1}{z - z_L} - \frac{1}{z - (r^2/\bar{z}_L)}\right] + \frac{\Gamma_R}{2\pi i}\left[\frac{1}{z - z_R} - \frac{1}{z - (r^2/\bar{z}_R)}\right] .$$

If we describe the flow by this velocity field and apply the same conditions as Bryson[5], *ie* that the velocity vector at the cone surface at each separation line lies along the separation line, and that the total force on each combination of a line-vortex and the cut joining it to its separation line is zero, then we have an extension of Bryson's model to asymmetric flow. Details may be found in Ref 4. Some results from using this model will be discussed in the next section.

To obtain the complete model, the contribution from the vortex sheets must be added to the expression above. For reasons discussed in Ref 3, special case is required in representing the vortex sheets. Specifically, the curvature of the vortex sheet at its base is, in general, infinite and must be regularised by means of a transformation that maps the cross-section of the cone at the sheet base into a right-angled concave corner. Because of the linear nature of the complex potential, each vortex sheet can be considered separately and so the problem reduces to the canonical one of finding the complex potential due to a single vortex sheet, and its image, leaving a circle tangentially and with infinite curvature. This is solved by first mapping the circular contour representing the cross-section of the cone onto the imaginary axis, with the region outside this contour being mapped onto the left half-plane. The origin is then shifted to the base of the vortex sheet (the separation position) and the axis system rotated. A folding (square root) transformation is then applied which maps the imaginary axis onto the positive parts of the real and imaginary axes and the right half-plane onto the first quadrant. See Fig 3. The construction of the velocity field then proceeds as explained in Ref 3, *ie* by representing the sheet as a collection of contiguous circular arcs, with continuous tangents at their junctions, in the final transformed plane, z_5 . Over each arc, a distribution of vorticity is specified (which is also continuous across the junctions) such that the velocity field for the sheet may be written in closed form. In effect, we have a panel method to represent the sheets.

The conditions that the vortex sheet forms a three-dimensional stream surface and that the pressure is continuous across it are applied at the points where the panels join, and at the mid-point of the panel nearest the core. The position and strength of a vortex panel are specified by one parameter each, so that these conditions are just sufficient to determine these unknowns. The position of each line-vortex is specified by two coordinates, so that requiring the two components of the total force on the vortex and the cut joining it to the free end of the sheet be zero provides equations determining the position of each vortex. The final unknowns are the circulation of the line-vortices. These are determined by the Kutta condition that the velocity vector at the base of each vortex sheet, between the sheet and the cone surface, lies along the separation line. The resulting set of non-linear algebraic equations is solved in an iterative manner, using a multi-dimensional analogue of the Newton-Raphson iteration method. In this method, a guess is made for each sheet shape, and its vorticity distribution, for given values of the incidence parameter and separation positions. This initial approximation is successively improved by the Newton method, until the boundary conditions on the vortex sheets are satisfied to within a specified error tolerance. Details may be found in Ref 3.

3 RESULTS

An obvious choice for an initial approximation to an asymmetric solution is one of the symmetric solutions found previously[3], and indeed, the first solutions for asymmetric vortex sheets were found by perturbing the symmetrical solutions. In particular, a gradually increasing asymmetry in the separation lines was introduced, and the resulting solutions found. A number of solutions were obtained, covering a wide range of separation positions. No attempt was made to use any particular values corresponding to experimentally observed separation positions at this stage - a range of values was taken in the hope of covering the likely range of experimental results. Of particular interest is the calculated side-force coefficient C_Y with asymmetric separation. In Fig 4, the values of the ratio C_Y to the normal force coefficient, C_N , are shown for a particular value, $\alpha/\delta = 3.5$, of the ratio of the angle of incidence, α , to the semi-angle of the cone, δ.

The abscissa is the difference in angular position between the separation lines on the port and starboard sides, so that the origin corresponds to zero C_Y with symmetrical separation lines. The two curves are for different fixed locations of the port separation lines. The most significant feature is that the value of C_Y/C_N is small, and never exceeds 0.09.

The values of C_Y/C_N measured on slender pointed bodies in general, and on circular cones in particular, depend on the orientation of the body in roll, and, in some experiments, the Reynolds number. The largest values of C_Y/C_N attained as the body is rolled about its axis are, of course, of the greatest interest. For circular cones, these maximum values depend mainly on the incidence parameter, α/δ . For the value of this parameter corresponding to the results shown in Fig 4 (3.5), the maximum values measured by Keener, *et al*[7] exceed 0.5. Since the range of separation positions covered in Fig 4 seems likely to include any occurring in a real flow, it is clear that these asymmetric solutions do not correspond to the observed phenomena.

If the solution to the inviscid flow problem were uniquely determined by the body shape, incidence and separation line positions, that would be the end of the matter. However, for such non-linear problems, there is always the possibility of non-unique solutions, although finding them may be difficult. The vortex sheet model is quite complex, and carrying out an extensive survey of its solutions would be a very time consuming process. So, the simpler line-vortex method was used to search for other possible solutions. As reported in Ref 4, the hunt for solutions alternative to those of the first family was successful, and a new family of solutions was found. In particular, asymmetric solutions were found for separation lines placed symmetrically about the incidence plane. These asymmetrical solutions with symmetric separation lines typify a distinct, second family of solutions; the solutions obtained by Bryson represent the first family. This classification into families can be extended to solutions with asymmetric separation lines, in an obvious way. For a particular value of the incidence parameter, a sequence of neighbouring solutions can be found (by the Newton-Raphson procedure) in which the positions of separation are varied. If the members of this sequence with symmetrical separation lines have symmetric vortices, then the whole sequence of solutions belongs to the first family. If not, and asymmetrical vortices are still found when the separation lines become symmetrical, then the sequence belongs to the second family of solutions. It turns out that solutions of the second family, defined in this way, give rise to values of C_Y/C_N approaching unity.

Some typical results are shown in Fig 5, where the locus of the vortex positions for varying incidence and fixed (symmetrical) separation positions. Two sets of results are plotted. Those labelled 1 are members of the first family of solutions and are symmetrical for all values of the incidence parameter, because the separation position is symmetrical. Those labelled 2 are examples of the second family, where the vortices are not symmetric. Fig 6 shows the corresponding results for C_Y/C_N calculated from the second family of line-vortex solutions. As can be seen, values similar to those observed in experiments (in this case, maximum values recorded during experiments by Keener, *et al*[7]), are obtained.

Eventually, for sufficiently large incidences, the results of the line-vortex model become physically unrealistic, with one vortex moving a very long way from the cone. Also, the Kutta condition used here merely enforces a crossflow stagnation point at the separation line position, but cannot ensure that the flow is away from the body at this point, *ie* a real separation line behaviour. In fact, at large incidences, the flow is found to attach at these points instead, which is another aspect of the physical unreality. Even at values of the incidence parameter which are of practical interest, the line-vortex model is unsatisfactory for several reasons. Most fundamentally, the possibility of determining the separation line in any rational way and without empiricism depends on a detailed representation of the flow near the separation line, as shown in Ref 3. Even in the present context, where we are treating the flow as inviscid, with prescribed separation lines, the predictions of the line vortex model are only qualitatively useful. The discrepancies between the line-vortex and the vortex sheet predictions for sharp-edged slender wings are familiar; they are greater for smooth bodies.

There is therefore a strong incentive to seek solutions for the vortex sheet model which correspond to the second family of solutions of the line-vortex model. There was also the hope that the line-vortex solutions would prove useful in finding the vortex sheet solutions. This eventually proved to be the case but not in any simple way. Details of the rather complex process used will be given in a later publication. For the present we confine ourselves to an examination of some typical results.

Fig 7 shows a symmetrical vortex sheet solution, for an incidence parameter of 3, and adjacent to it an asymmetric solution for the same incidence parameter and the same symmetric separation positions. Hence this asymmetric solution is a member of the second family of solutions, while the symmetric solution is a member of the first family. The different extent of the outer part of the vortex sheet in the two solutions is not thought to be significant. The vortex which lies closer to the surface is very similar in shape to the symmetrical vortices. The farther vortex is very different with a long length of almost straight sheet, rolling up at its free edge, rather like the trailing vortex sheet from a slender delta wing at very large angles of yaw (see Jones[8]). Also shown as small circles are the positions of the vortices in the corresponding solution of the line-vortex model, *ie* for the same incidence parameter and separation line locations. It is apparent that these vortices do not in any way represent the core position of the vortex sheet

solution as had been hoped. Further examination of the vortex sheet solution reveals that the bulk of the circulation resides on the portion of the sheet represented explicitly - not in the core itself. This is particularly marked for the farther vortex. Consequently, in going from the line-vortex solution to the vortex sheet, a major re-distribution of circulation takes place, as well as a large shift in core position.

Peake, Owen and Johnson report some experimental results for the asymmetric flow over a circular cone in Ref 9. Included in their results are vapour screen photographs of a cross-section of the flow, showing the two primary vortex cores. It is interesting to make a qualitative comparison between one of these vapour screen photographs (Fig 8) and a calculated vortex sheet for a similar configuration (Fig 7). Note that the observed asymmetric flow has one vortex core much higher than the other, and both cores lie close to the incidence plane, as predicted by the vortex sheet model.

In order to make a comparison with experimental side-force data, we choose recent measurements made by Mundell at RAE[2]. He has appreciated the importance of rigid model mounting and of making a thorough investigation of roll angle dependence from the work of Hunt and Dexter[10] on ogive-cylinders. In addition, there are two features of his experiment which make his results particularly suitable for comparison with the predictions of the present theoretical model. The wind tunnel model (Fig 9) consists of a conical nose blended smoothly into a cylindrical afterbody. The model is constructed in two portions and the forces on the front portion are measured separately. This portion is conical and sufficiently far forward of the blending section for the flow over it to be very nearly conical, even at the low speeds of his experiment. The second feature is that, at flow speeds of up to 50 m/s, the boundary layers on the conical nose are laminar at separation, so that the separation line is almost straight. Mundell established that the side force for a given incidence changed sign as the roll angle varied, but that the absolute value of the side force was almost the same over most of the roll angle range. In order to reproduce this level without the need for roll angle variation, he fixed the behaviour of the side force by introducing a small protuberance at the apex of the cone. This had a negligible effect on the magnitude of the side force and also made it possible to measure the separation line positions which correspond to the side-force values, using an oil flow technique. It is thus possible to compare Mundell's experimental results and the predictions of the vortex sheet model in some detail. We shall concentrate on a comparison of the maximum side force at a particular incidence, 36 degrees. For this case, Mundell measured separation positions at 0 degree and 166 degrees. It is interesting to note that this asymmetry in separation position is only 14 degrees. These separation positions were used to calculate vortex-sheet solutions for an incidence parameter of 3.6 (Mundell's cone had a 10 degree semi-apex angle). Two solutions were found, one from the first family, and one from the second. They are shown in Fig 10. It can be seen that the solution from the first family is only slightly asymmetric, in contrast to the marked asymmetry of the second family solution. Comparison with the solutions of Fig 7 shows that the large values of the incidence parameter and the earlier separation have resulted in larger vortices, as would be expected. At the same time, there is a clear 'family' resemblance between the solutions for the two cases, despite the asymmetry in the separation position in Fig 10. A further comparison of the two solutions is given below, in tabular form:

		First family	Second family	Expt.
Γ_{total}	left	-13.73	-13.86	
	right	16.01	14.02	
$\Gamma_{core}/\Gamma_{total}$	left	0.64	0.80	
	right	0.60	0.25	
C_Y/δ^2		-1.53	-19.73	-17.6
C_N/δ^2		36.81	36.75	27.0

We note first that the strengths of all the vortices are similar, and, in particular, that the very different looking vortices of the second family have almost the same strength. The next line of the table gives a simple comparison of the way in which the circulation is distributed in the vortex. Γ_{core} is defined as the circulation of the isolated vortex plus the circulation of the portion of the sheet which lies beyond its highest point. There is little difference in the distribution for the vortices of the first family solution: but in the second family we see that the nearer vortex, on the left, has the bulk of its circulation in the core, while the further vortex, on the right, has the bulk of the circulation in the sheet.

The force coefficients are based on the free-stream kinetic pressure and the plan area of the model back to its split line, and the tabulated quantities are further divided by the square of the semi-angle of the cone (in radians), to give similarity variables. As expected, the side force from the first family is smaller than the measured value by an order of magnitude. The solution from the second family gives an approximation to the measured value which is surprisingly close, considering the assumption of small incidence which is inherent in slender-body theory. There can be little doubt that the second family corresponds to the observed flow. The solution of both families predict much the

same level of normal force, which is much greater than that measured. This is a reflection of the limitations of the small incidence assumption implicit in slender-body theory. Figs 11 and 12 show pressure distributions round the surface of the cone for the calculated solutions shown in Fig 10. The independent variable, θ' , is the angular position measured from the windward generator. The ordinate is the difference between the local pressure coefficient and its value at the windward generator, converted to a similarity form by division by δ^2 . In the solution from the first family, Fig 11, two suction peaks can be seen on each side of the cone. The first is related to the maximum of the circumferential velocity from windward to leeward which occurs near the equatorial position. The pressure rise following this suction peak leads to the flow separation, following which the pressure is initially almost uniform. The second, much larger, suction peak follows, corresponding to a maximum in the circumferential velocity from leeward to windward under the vortex core. In a real flow the second peak would be modified by the effects of secondary separation in a similar way to that observed on delta wings. In this solution from the first family, the dominant contribution to the side force comes from the difference between the first peaks on the two sides of the body. The contribution from the second peaks is smaller, because the lateral projection of the surface element on which it acts is much smaller.

In the solution from the second family, shown in Fig 12, the most striking feature is the absence of any suction peak related to the farther vortex core shown in Fig 10. At the same time, the suction peak of the nearer core is much enhanced, as is the suction peak preceding separation on the side where the core is nearer. The side force is consequently much larger for the second family, in agreement with the overall forces presented earlier. Another feature of the increased asymmetry of the solution of the second family is the displacement of the leeward attachment line by some 20 degrees from the leeward generator. The positions of the other attachment and separation lines are also indicated in Figs 11 and 12.

The results presented here are very much those of 'work in progress', and a more extensive survey of the second family of vortex sheet solutions is needed. In particular, it should be possible to discover for what range of incidence parameter and separation positions the second family of solutions exists, and whether they can be related to the first family in any way.

Such a survey has already been conducted with the simpler line-vortex model. Here, the second family of solutions are found to arise from the first family by a process of bifurcation. This is illustrated in Fig 13, where the coordinates of the vortex are shown as functions of the incidence parameter, the separation positions being fixed symmetrically. The curves labelled 'symmetric' represent the solution for the first family. For symmetric separations, these are Bryson's solutions, which start, with a vertical tangent, where $\alpha/\delta = 1.5 \operatorname{cosec} \theta \simeq 1.81$. At a value of the incidence parameter just above 2, at the point labelled B , the asymmetric solutions depart from the symmetric solution along a vertical tangent, in opposite directions. When attempting to calculate the solutions, it is important to consider that the determinant of the Jacobian matrix, on which the Newton scheme depends, vanishes at B . We see from Fig 13 that the second family of solutions for the line-vortex model does not exist for all combinations of separation position and incidence parameter. Fig 14 shows, for symmetrically placed separation lines, $(\theta_1 + \theta_2 = 180$ degrees), two boundaries in the plane of incidence parameter α/δ , and separation position, θ_1 . The first is the boundary, found by Bryson[5] below which there are no solutions for the first family with the vortices near the surface of the cone. The second is the bifurcation boundary, below which no asymmetric, second family solutions are found. It is plausible that similar boundaries for the existence of solutions of the vortex sheet model falling into the first and second families exist, but more work is needed to establish them. We note that symmetric vortex sheet solutions are found in Ref 3 at values of the incidence parameter which are below the lower limit for solutions of the line-vortex model.

4 CONCLUSIONS

It is important to recall the limitations and approximations of the present approach to the problem of out-of-plane forces on bodies. In the first place, attention has been concentrated on the maximum levels of side force which occur. Secondly, consideration has been confined to circumstances in which separation along the body sides extends all the way forward to the pointed apex of the body, in other words, for angles of incidence which are large in terms of the semi-angle of the apex. Out-of-plane forces also arise in other circumstances, for instance through separation on cylindrical afterbodies. For flows which do separate from the apex, the present treatment is confined to circular cones, though it could readily be extended both to cones of other cross-sections and to non-conical bodies. However, the limitations inherent in slender-body theory would have to be borne in mind in any attempt to make use of its quantitative predictions in aerodynamic design.

What is claimed for the present treatment is that it reveals an inviscid mechanism - namely the existence of multiple inviscid solutions to a simple, well-defined problem - which can give rise to flows and forces which are close to those observed, the results suggest that this mechanism is responsible for the occurrence of out-of-plane force on the whole class of pointed bodies under conditions in which separation extends to the apex, though the downstream development of the flow will inevitably be much more complicated than the conical structure assumed here.

REFERENCES

1 L.E. Ericsson and J.P. Reding: "Slender and unsteady vortex-induced loads on slender vehicles." J. Spacecraft and Rockets, 18, 97-109 (1981)

2 A.R.G. Mundell: RAE Unpublished (1982)

3 S.P. Fiddes: "A theory of the separated flow past a slender elliptic cone at incidence." Paper 30 in 'Computation of Viscous-Inviscid Interactions', AGARD CP 291 (1980)

4 D.E. Dyer, S.P. Fiddes and J.H.B. Smith: "Asymmetric vortex formation from cones at incidence - a simple inviscid model." RAE Technical Report 81130 (1981)

5 A.E. Bryson: "Symmetrical vortex formation on circular cylinders and cones." J. Appl. Mech. (ASME) 26, 643-8 (1959)

6 J.H.B. Smith: "Improved calculations of leading-edge separation from slender delta wings." RAE Technical Report 66070 (1966)

7 E.R. Keener, G.T. Chapman, L. Cohen and J.T. Taleghani: "Side-forces on fore-bodies at high angles of attack and Mach numbers from 0.1 to 0.7; two tangent ogives, paraboloid and cone." NASA TM X-3438 (1977)

8 I.P. Jones: "Flow separation from yawed delta wings." Computers and Fluids, 3, 155-177 (1975)

9 D.J. Peake, F.K. Owen and D.A. Johnson: "Control of forebody vortex orientation to alleviate side-forces." AIAA Paper 80-0183 (1980)

10 B.L. Hunt and P.C. Dexter: "Pressures on a slender body at high angle of attack in a very low turbulence level air stream." Paper 17 in 'High Angle of Attack Aerodynamics', AGARD CP 247 (1979)

Figs 1-3

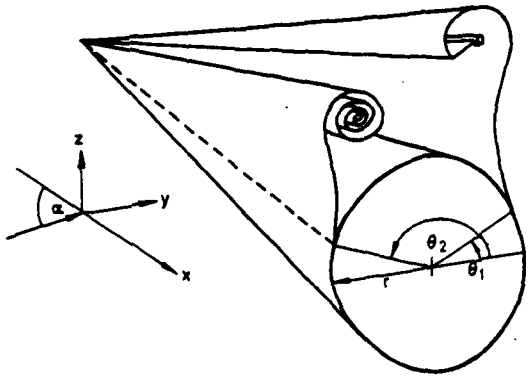

$r(x) = \delta x$

Fig 1 Coordinate system

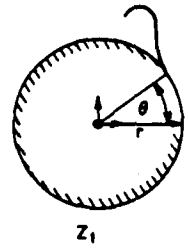

Z_1

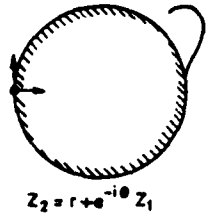

$Z_2 = r + e^{-i\theta} Z_1$

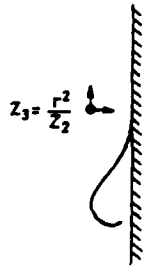

$Z_3 = \frac{r^2}{Z_2}$

$Z_4 = \frac{r}{2} - Z_3$

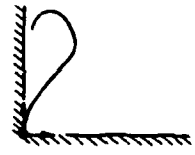

$Z_5 = \sqrt{2ir Z_4}$

Fig 3 Transformation sequence

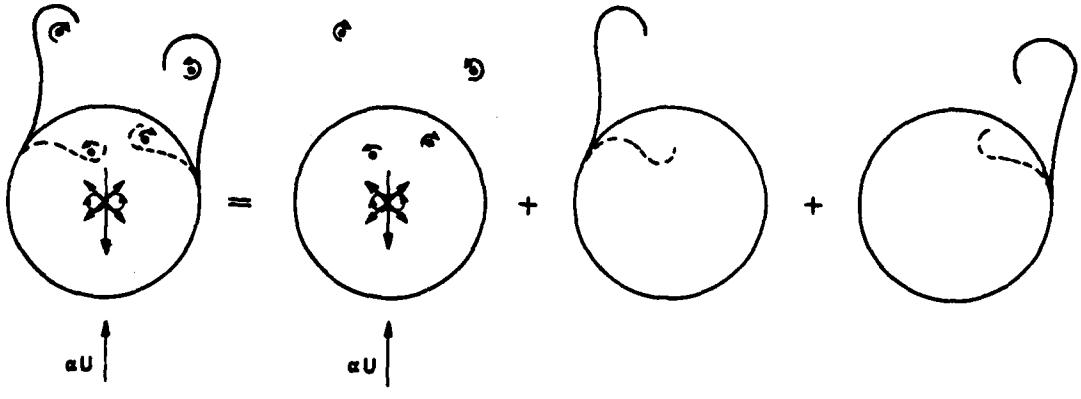

Complete velocity field	is composed of	Source and dipole, point vortices (and images)	Left hand vortex sheet (and image)	and	Right hand vortex sheet (and image)

Fig 2 Components of velocity field

Figs 4-8

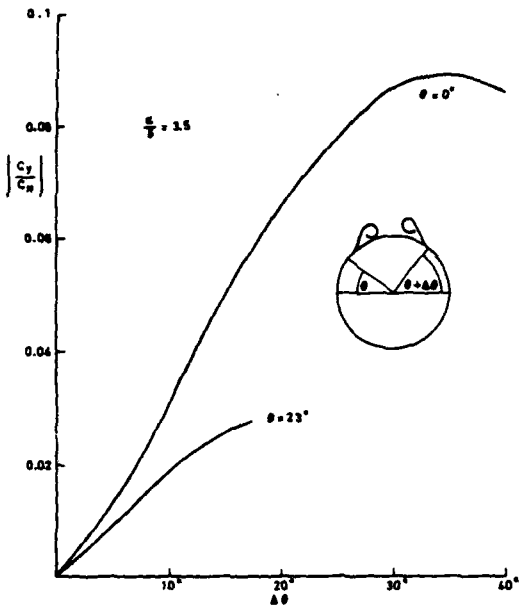

Fig 4 Side force induced by asymmetrical separation positions

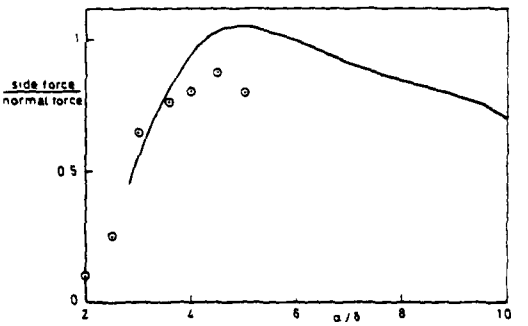

Fig 6 Ratio of side force to normal force on cone: line-vortex model calculations for $\theta_1 = 40°$, $\theta_2 = 140°$, and measurements of Keener *et al* (Ref 7)

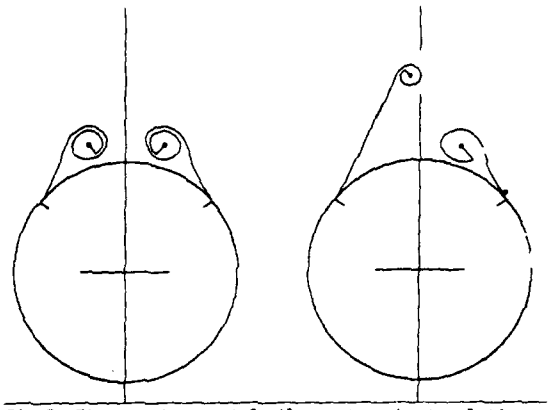

Fig 7 First and second family vortex sheet solutions for symmetric separation; $\alpha/\delta = 3.0$, $\theta_1 = 40°$, $\theta_2 = 140°$

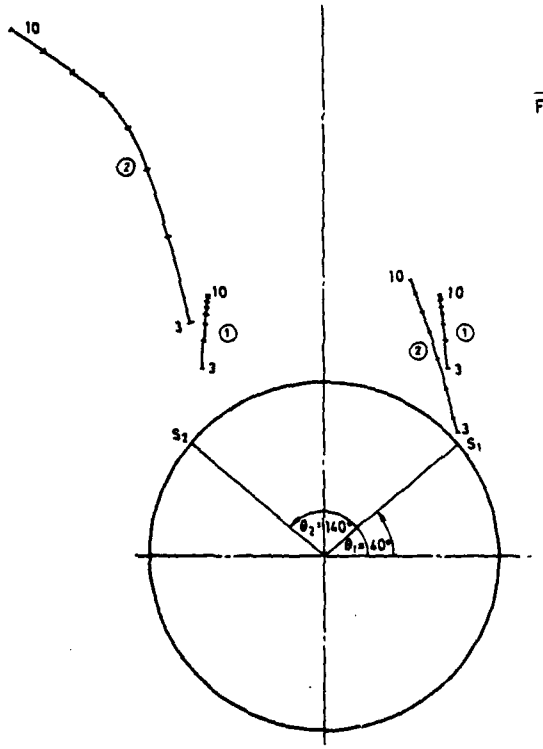

Fig 5 Symmetrical and asymmetric line-vortex positions for symmetric separation and $\alpha/\delta = 3(1)10$
1 = first family; 2 = second family

VIEW FROM BEHIND CONE BASE

$\alpha/\delta = 3.2$

Fig 8 Vapour-screen photograph of asymmetrical flow (from Ref 8)

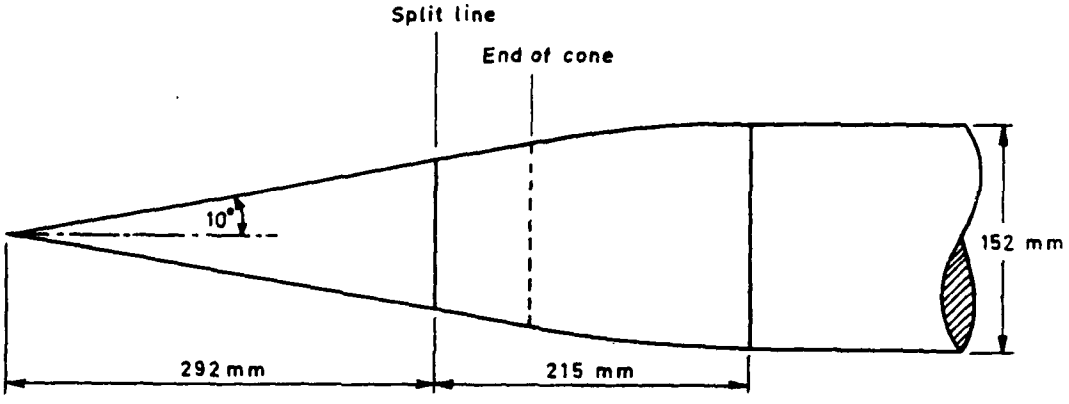

Fig 9 Cone model used by Mundell (Ref 2)

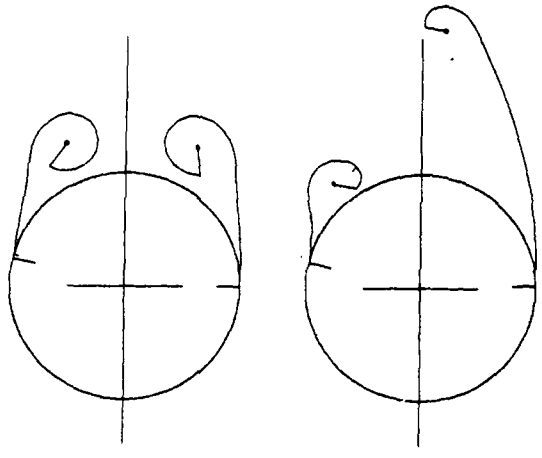

Fig 10 First and second family vortex sheet solutions for $\alpha/\delta = 3.6$, $\theta_1 = 0^\circ$, $\theta_2 = 166^\circ$

Figs 11&12

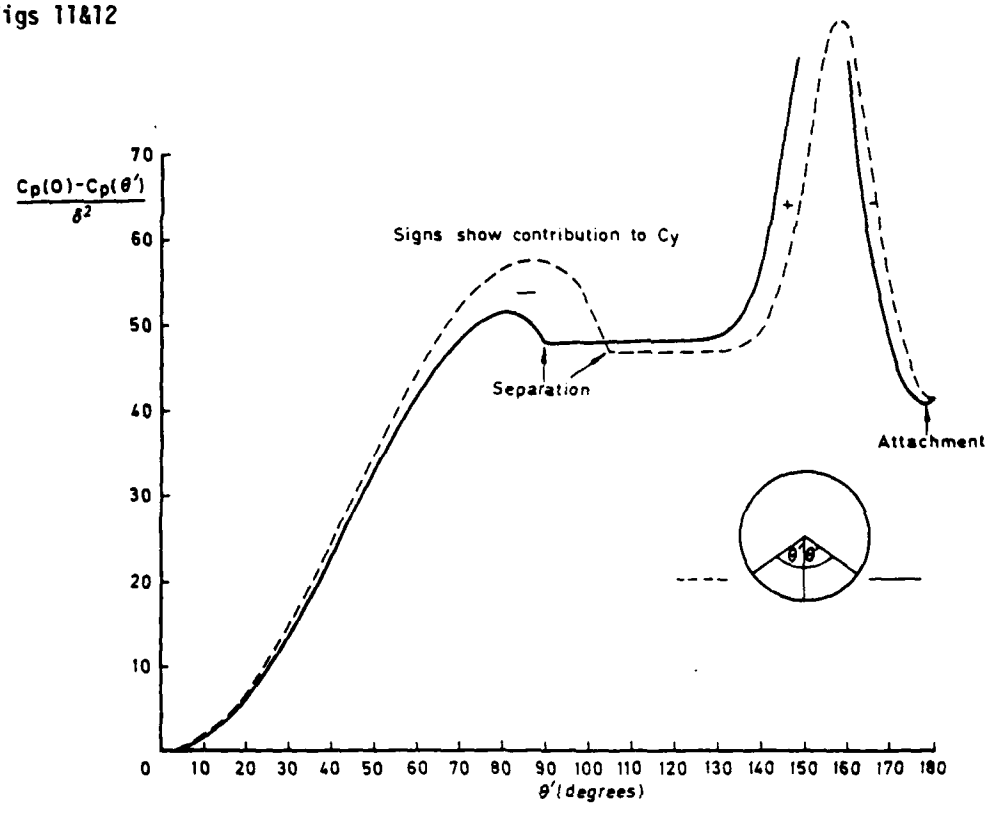

Fig 11 Pressure distribution for first family solution of Fig 10

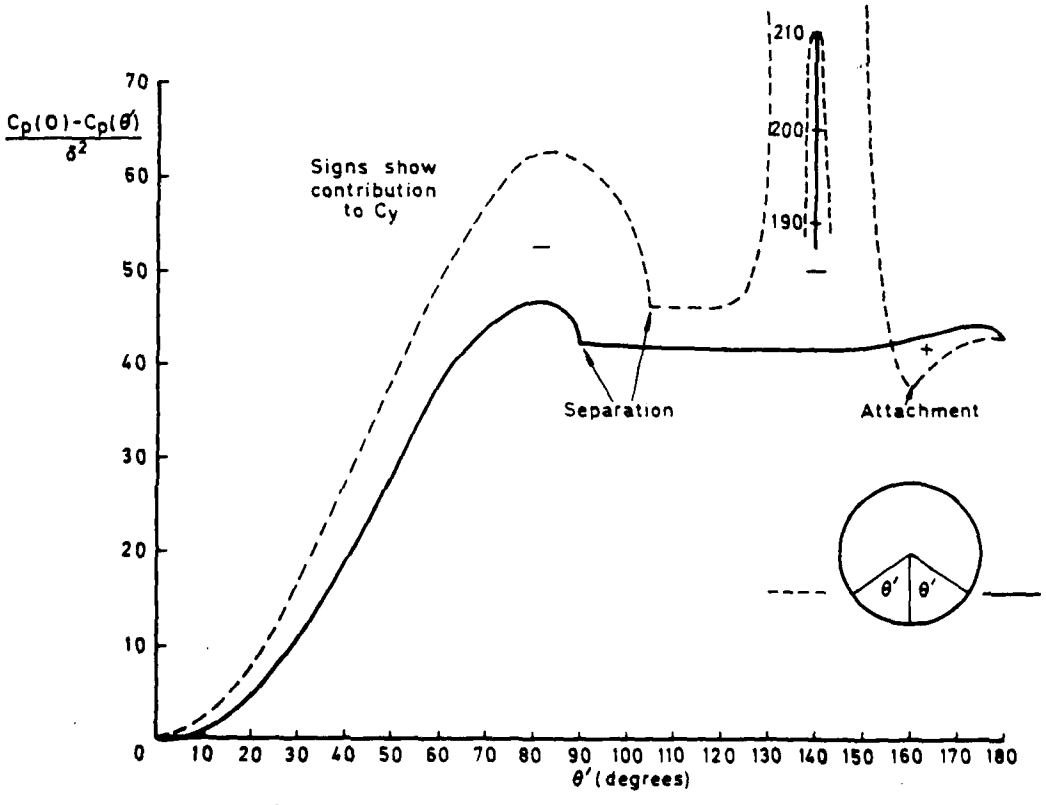

Fig 12 Pressure distribution for second family solution of Fig 10

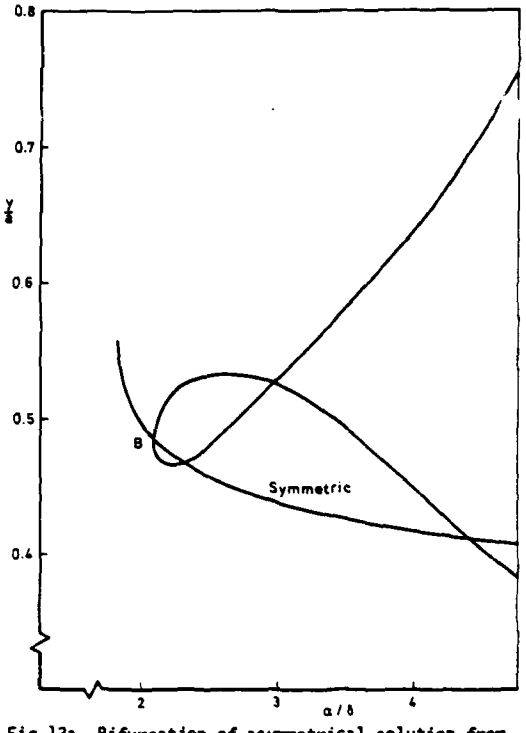

Fig 13a Bifurcation of asymmetrical solution from symmetrical solution, $\theta_1 = 56°$, $\theta_2 = 124°$, Lateral position of vortices from line-vortex model

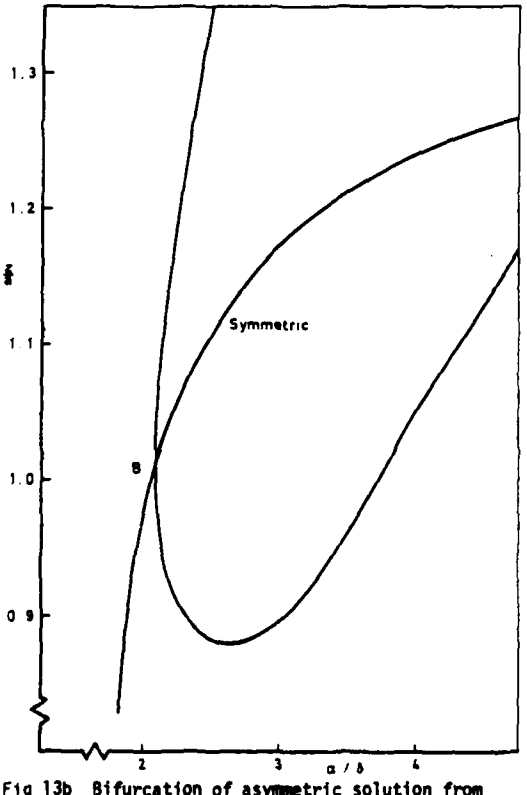

Fig 13b Bifurcation of asymmetric solution from symmetrical solution, $\theta_1 = 56°$, $\theta_2 = 124°$, vertical position of vortices from line-vortex model

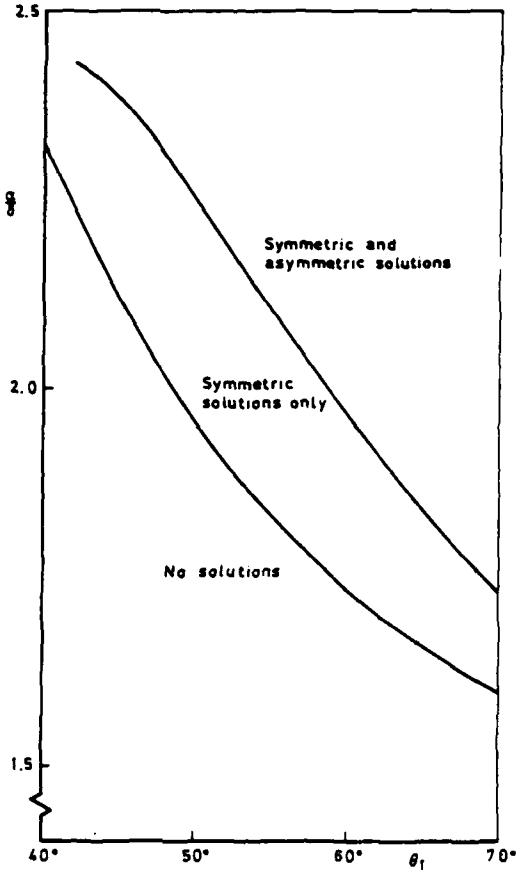

Fig 14 Regions of parameter plane in which solutions exist: $\theta_1 + \theta_2 = 180°$

REPORT DOCUMENTATION PAGE

Overall security classification of this page

UNLIMITED

As far as possible this page should contain only unclassified information. If it is necessary to enter classified information, the box above must be marked to indicate the classification, e.g. Restricted, Confidential or Secret.

1. DRIC Reference (to be added by DRIC)	2. Originator's Reference	3. Agency Reference	4. Report Security Classification/Marking
	RAE TM Aero 1949	N/A	UNLIMITED

5. DRIC Code for Originator	6. Originator (Corporate Author) Name and Location
7673000W	Royal Aircraft Establishment, Farnborough, Hants, UK
5a. Sponsoring Agency's Code	**6a. Sponsoring Agency (Contract Authority) Name and Location**
N/A	N/A

7. Title: Calculations of asymmetric separated flow past circular cones at large angles of incidence

7a. (For Translations) Title in Foreign Language

7b. (For Conference Papers) Title, Place and Date of Conference

Missile Aerodynamics; Trondheim, 20-22 September 1982

8. Author 1. Surname, Initials	9a. Author 2	9b. Authors 3, 4....	10. Date	Pages	Refs.
Fiddes, S.P.	Smith, J.H.B.	-	June 1982	13	10

11. Contract Number	12. Period	13. Project	14. Other Reference Nos.
N/A	N/A		

15. Distribution statement

(a) Controlled by – Head of Aerodynamics Department

(b) Special limitations (if any) –

16. Descriptors (Keywords) (Descriptors marked * are selected from TEST)

Vortices*. Boundary-layer separation*. Slender bodies*. Side force.

17. Abstract

The results of calculations of the flow over slender circular cones at large angles of incidence are presented. The vortices which form above the cone as a result of boundary-layer separation are represented by two inviscid models: as isolated line-vortices and as vortex sheets with line-vortex cores. For each model, an essentially new family of solutions is revealed, in which the flow remains asymmetric even when the separation lines are specified to lie symmetrically about the incidence plane. The side force which is predicted by this second family of solutions is very much larger than the side force which can be obtained by specifying asymmetric separation lines in the first family of solutions, and corresponds to the maximum side-force levels found experimentally. It is concluded that an essentially inviscid mechanism for the generation of side force at zero yaw has been discovered.

END

DATE
FILMED

10-82

DTIC